Available at
www.ElsevierMathematics.com
POWERED BY SCIENCE DIRECT®

ELSEVIER

Applied Numerical Mathematics 47 (2003) 91–108

APPLIED NUMERICAL MATHEMATICS

www.elsevier.com/locate/apnum

# CGLS-GCV: a hybrid algorithm for low-rank-deficient problems

Fermín S.V. Bazán [1]

*Department of Mathematics, Federal University of Santa Catarina, 88040-900 Florianópolis, SC, Brazil*

**Abstract**

Given $\widetilde{A} = A + E \in \mathbb{C}^{m\times n}$, where $\operatorname{rank}(A) \ll \min(m,n)$, and $\tilde{b} = b + \varepsilon$, we investigate the following problems: (a) the construction of approximate minimum norm solutions of the least squares problem $\min \|Ax - b\|$, and (b) the computation of approximations of the column (row) subspace of $A$. We propose an algorithm for solving these problems based on conjugate gradient iterations followed by regularization in the generated Krylov subspace. Regularization is introduced for estimating $\operatorname{rank}(A)$ and implemented using the generalized cross-validation technique. We report the outcome of numerical experiments, showing that the new algorithm yields results with accuracy comparable to that of the SVD, but at a lower computational cost.


*Keywords:* Rank-deficient problems; Iterative methods; Signal reconstruction

## 1. Introduction

Rank-deficient problems appear in a number of areas such as biology, physics, and engineering. They involve systems of linear equations in which the coefficient matrix has a cluster of small singular values and there (hopefully) exists a well-determined gap in the singular value spectrum [18, p. 2]. A basic assumption is that the coefficient matrix is often regarded as the result of perturbing an *exactly* rank-deficient matrix, i.e.,

$$\widetilde{A} = A + E \in \mathbb{C}^{m\times n}, \tag{1.1}$$

where both $A$ and $E$ are unknown, $E$ contains random noise, and $\operatorname{rank}(A) = r \ll \min(m,n)$ is also unknown. In applications such as signal processing, $A$ is an ideal covariance matrix (positive semidefinite Hermitian), and the available data matrix $\widetilde{A}$ approximately satisfies the low-rank-plus-shift structure

$$\widetilde{A} \approx A + \gamma I, \quad \gamma > 0, \tag{1.2}$$

*E-mail address:* fermin@mtm.ufsc.br (F.S.V. Bazán).

[1] This research was sponsored by CNPq, Brasil, Grant 300487/94-0(NV).

0168-9274/$30.00 © 2003 IMACS. Published by Elsevier B.V. All rights reserved.
doi:10.1016/S0168-9274(03)00060-6

where $I$ is the identity matrix and $\gamma$ is the noise variance [27]. This same property is also encountered in information retrieval when the cross product of term-document matrices is formed [28]. Many other problems involving rank-deficient matrices are also encountered in modal analysis and time domain analysis of nuclear magnetic resonance (NMR) signals, see [2,11,25,26].

Henceforth, unless otherwise stated, $A$ will always denote a rank-deficient matrix in $\mathbb{C}^{m\times n}$; its column subspace $\mathcal{R}(A)$ will be denoted by $\mathcal{S}$ and its row subspace $\mathcal{R}(A^*)$ by $\mathcal{S}'$. The conjugate transpose of $A$ is denoted by $A^*$. We will always assume that the nonzero singular values of $A$ are simple.

Assuming $\widetilde{A} = A + E$ and $\tilde{b} = b + \varepsilon$ as input data, we shall be concerned with: (a) the construction of approximate minimum norm solutions of the unperturbed least squares (LS) problem

$$\min \|Ax - b\|_2, \quad A \in \mathbb{C}^{m\times n}\ (m \geqslant n),\ b \in \mathbb{C}^m, \tag{1.3}$$

and (b) the computation of approximations of the column (row) subspace of $A$. In the sequel these will be referred to as problems P1 and P2, respectively.

An important issue regarding P1 and P2 is that their solutions strongly depend on a correct estimation of the rank of the unperturbed matrix from the available data. This estimation is problem dependent and becomes very difficult at high noise levels. However, a number of schemes to circumvent this drawback are available, most of which may be found in system identification and signal processing; see, for instance, the numerous references in [7] and [24]. The inconvenience of these schemes is that they require either doing full eigenvalue (singular value) decompositions, which is computationally demanding, or the presence of a well distinct gap in the singular spectrum. Cheaper alternatives to the SVD are the so-called rank-revealing (RR) decompositions. These, however, also require a large gap in the singular spectrum [12], [18, p. 46]. For applications of RR-based techniques in NMR, see [11,26].

In this work, a method for solving problems P1 and P2 is introduced, which is designed to avoid the SVD as well as to address the rank estimation problem, even in those cases where the singular spectrum presents no clear gap. The CGLS-GCV algorithm presented herein relies on a combination of the conjugate-gradient (CG) method for LS problems (CGLS) [5, p. 289] with regularization in the generated Krylov subspace. Specifically, we perform a few CGLS iterations and then construct a small least squares problem by projecting the original one onto the generated Krylov subspace. Solutions to P1 and P2 emerge after solving this small problem using regularization, by truncating the SVD of the resulting matrix. Regularization is introduced to estimate $\operatorname{rank}(A)$ and implemented using the generalized cross-validation (GCV) technique of Golub, Craven, and Wahba [13]. Methods of this kind, sometimes called hybrid methods [18, Section 6.6], were first introduced in [21], in 1981. Since then, several hybrid methods have been successfully applied to solve large-scale ill-conditioned problems. However, no works are known to the author that illustrate the use of these methods in solving exactly rank-deficient problems from noisy data.

In this work, we show by way of numerical experiments that the proposed algorithm handles the rank detection problem relatively well, without requiring the presence of a distinct gap in the singular spectrum of the data matrix. Additionally, the algorithm is shown to yield solutions to P1 and P2 with accuracy comparable to that of the SVD, but at a lower computational cost. The application we have in mind is harmonic retrieval.

The rest of the paper is organized as follows. Section 2 reviews the basic philosophy of GCV for solving discrete ill-posed problems via truncation of the singular spectrum of the data matrix, including a discussion that motivates the use of GCV on rank-deficient problems. The proposed method as well as a stopping criterion for CGLS in harmonic retrieval are described in Section 3. Finally, in Section 4, the

results of numerical experiments are presented which illustrate the efficiency of CGLS-GCV for solving difficult rank-deficient problems taken from the NMR field. Furthermore, a numerical comparison is provided which shows the superiority of our algorithm in terms of computational cost and accuracy over those obtained by RR algorithms.

## 2. Review of GCV for TSVD

We first consider LS problems of the form

$$\min \left\| Ax - \tilde{b} \right\|_2, \quad A \in \mathbb{C}^{m\times n} \ (m \geqslant n), \ \tilde{b} \in \mathbb{C}^m, \tag{2.4}$$

where the right hand side $b$ is affected by errors: $\tilde{b} = b + \varepsilon$ ($\varepsilon$ stands for random noise), and $A$ is of full rank but free of errors. Let the SVD of $A$ be

$$A = U \Sigma V^* = \sum_{j=1}^{n} \sigma_j u_j v_j^*, \tag{2.5}$$

where $\sigma_j > 0$, $j = 1, \ldots, n$, with $u_j$ and $v_j$ being the left and right singular vectors of $A$. Then the solution $x_{\mathrm{LS}}$ to the LS problem (2.4), using the available data $\tilde{b}$, is given by

$$x_{\mathrm{LS}} = \sum_{j=1}^{n} \frac{u_j^* \tilde{b}}{\sigma_j} v_j.$$

When the coefficient matrix $A$ arises from discretization of ill-posed problems, both $\sigma_j$ and the coefficients $u_j^* b$ decay gradually (sometimes rapidly) to zero. In this case, it is clear that the solution $x_{\mathrm{LS}}$ will be dominated by the errors, since, for indices $j$ where $u_j^* b \approx 0$, the coefficients

$$\frac{u_j^* \tilde{b}}{\sigma_j} = \frac{u_j^* b}{\sigma_j} + \frac{u_j^* \varepsilon}{\sigma_j} \approx \frac{u_j^* \varepsilon}{\sigma_j},$$

become arbitrarily large due to the small singular values. This difficulty can be circumvented by using the truncated SVD (TSVD) method, which consists of constructing approximate solutions of the form

$$x_k = \sum_{j=1}^{k} \frac{u_j^* \tilde{b}}{\sigma_j} v_j, \tag{2.6}$$

where the *truncation* (*regularization*) *parameter* $k$ depends on the noise level $\varepsilon$, and has to be chosen so that the noise contribution is damped out.

There exist different ways of choosing the regularization parameter [18]. Here we employ the GCV technique, which suggests choosing as regularization parameter the index $k$ that minimizes the GCV function

$$G(k) = \frac{\|A x_k - \tilde{b}\|_2^2}{\mathrm{tr}(I - A A_k^{\dagger})^2}, \quad k = 1, 2, \ldots, \tag{2.7}$$

where $x_k$ is a TSVD solution, $A_k^{\dagger}$ is the pseudo inverse of the closest rank-$k$ approximation of $A$, and $\mathrm{tr}(A)$ denotes the trace of $A$. This choice has the advantage that no a priori information on the noise level is required, and it works well in practice.

In order to better understand how GCV works, the GCV function is rewritten in terms of the SVD of $A$ as in [6]:

$$G(k) = \left(\frac{1}{n-k}\right)\left(\frac{\sum_{j=k+1}^{n} |u_j^* \tilde{b}|^2}{n-k}\right), \quad k = 1, 2, \ldots. \tag{2.8}$$

We now make the crucial observation that random noise vectors tend to have a constant projection along all singular vectors $u_j$. From this, because we deal with a discrete ill-posed problem, there exists a integer $k_*$ such that

$$\left|u_j^* \tilde{b}\right| = \left|u_j^* b + u_j^* \varepsilon\right| \approx \left|u_j^* \varepsilon\right| \approx \text{constant} \quad \text{for } j > k_*. \tag{2.9}$$

Thus, for $j > k_*$, the right factor in (2.8) behaves approximately as a constant that serves as a variance estimate for the random vector $\varepsilon$. As a consequence, for $k > k_*$, $G(k)$ starts increasing because of the "weight" $1/(n-k)$, and the GCV function is not minimized for $k$ in this range. On the other hand, when $1 \leqslant k < k_*$, large coefficients $|u_j^* \tilde{b}|$ enter into the variance estimate and the minimum of the GCV function is not achieved in this interval. The GCV function should thus be minimized at $k = k_*$.

To end our review of GCV, notice that, if (2.9) holds, then the variance estimate based on the last $n - k_*$ coefficients should not depart so much from other variance estimates based on coefficients $|u_j^* \tilde{b}|$, with $j$ running from $k_* + 1$ to $\hat{n}$, where $\hat{n} \lesssim n$. This suggests that, if we define an alternative GCV function $\widehat{G}(k)$ by simply replacing $n$ with $\hat{n}$ in (2.8), this GCV function should also be minimized at $k = k_*$. Function $\widehat{G}(k)$ can be useful when some of the last coefficients are inaccurately computed; it will be referred to as a *restricted* GCV function. For further details regarding the GCV, see [6].

We shall now discuss the use of GCV in the context of rank-deficient problems. Recall that our interest is to construct approximate solutions for problems P1 and P2 from data $\widetilde{A} = A + E \in \mathbb{C}^{m\times n}$, $\tilde{b} = b + \varepsilon \in \mathbb{C}^m$, where $A$ is rank-deficient with $\operatorname{rank}(A) \ll \min(m, n)$. For our discussion, we shall need to analyze the SVD-based solution to P1. Let $\widetilde{A}$ have an SVD given by

$$\widetilde{A} = \widetilde{U}\,\widetilde{\Sigma}\,\widetilde{V}^* = \sum_{j=1}^{n} \tilde{\sigma}_j \tilde{u}_j \tilde{v}_j^*, \tag{2.10}$$

and assume that $r = \operatorname{rank}(A)$ is available. An approximation of the exact solution to P1, $x^\dagger = A^\dagger b$, is then given by

$$\tilde{x}_{\text{SVD}} = \sum_{j=1}^{r} \frac{\tilde{u}_j^* \tilde{b}}{\tilde{\sigma}_j} \tilde{v}_j, \tag{2.11}$$

whereas $\widetilde{\mathcal{S}} = \operatorname{span}\{\tilde{u}_1, \ldots, \tilde{u}_r\}$ is an approximate solution to P2. Notice that these solutions are of theoretical interest only. In practice, the SVD has to be substituted for a less computationally demanding technique and $r$ has to be estimated during the computation. The algorithm we propose addresses the rank-estimation problem by minimizing an appropriate GCV function to be described later. The motivation to use GCV comes from the observation that it is possible to find practical applications in which the coefficients $\tilde{u}_j^* \tilde{b}$ behave as in (2.9) for $j > r$. This is an important observation since, according to the review above, the associated GCV function should be minimized at $k_* = r$. That is, GCV should satisfactorily estimate $\operatorname{rank}(A)$. As an example, if $\widetilde{A}$ is as in (1.2) (which often happens in signal processing), and the unperturbed vector $b$ lies in $\mathcal{S}$, then $\tilde{u}_j^* \tilde{b} \approx u_j^* b + u_j^* \varepsilon \approx u_j^* \varepsilon$ for $j > r$, because in this case the singular vectors are almost preserved and $u_j \in \mathcal{S}^\perp$ for $j > r$. Hence, since the

(crucial) condition (2.9) is met for $k > r$, the associated GCV function should estimate $\operatorname{rank}(A)$. The case $b \notin \mathcal{S}$ can be worked out in a similar fashion if one chooses an auxiliary "right hand side" having strong components on $\mathcal{S}$. One could choose, for instance, $\breve{b} = \widetilde{A}e_1$, where $e_1$ is the first canonical vector of $\mathbb{R}^n$. When (1.2) is not a good model for $\widetilde{A}$, difficulties appear. But, if $\tilde{b}$ has stronger components in the approximate subspace $\widetilde{\mathcal{S}}$ than in its orthogonal complement $\widetilde{\mathcal{S}}^{\perp}$, we can expect $G(k)$ to be minimized at $k = r$. Another alternative, which we exploit later, is to minimize a GCV function that analyzes the components of $\widetilde{A}^*\tilde{b}$ on right singular vectors. Details are postponed to Section 3.

The preceding discussion suggests we perform an analysis of the behavior of the coefficients $\tilde{u}_j^*\tilde{b}$, which is done in the sequel. Some definitions and one lemma will be needed. The distance between subspaces $\mathcal{S}_1$ and $\mathcal{S}_2$ of the same dimension is defined by $\mathrm{d}(\mathcal{S}_1, \mathcal{S}_2) = \sin(\theta_1)$, where $\theta_1$ is the largest canonical angle between $\mathcal{S}_1$ and $\mathcal{S}_2$; see [5, p. 18] for details. We also define

$$\cos\Theta = \operatorname{diag}\big(\cos(\theta_1), \ldots, \cos(\theta_r)\big), \qquad \sin\Theta = \operatorname{diag}\big(\sin(\theta_1), \ldots, \sin(\theta_r)\big), \tag{2.12}$$

with the canonical angles ordered so that $\theta_1 \geqslant \theta_2 \geqslant \cdots \geqslant \theta_r$.

**Lemma 1.** *Assume that $\widetilde{A}$, $A$ given in* (1.1) *have SVD's*: $A = [U_1 U_2]\operatorname{diag}(\Sigma_1, \Sigma_2)[V_1 V_2]^*$ *and* $\widetilde{A} = [\widetilde{U}_1 \widetilde{U}_2]\operatorname{diag}(\widetilde{\Sigma}_1, \widetilde{\Sigma}_2)[\widetilde{V}_1 \widetilde{V}_2]^*$, *where $U_1$, $\widetilde{U}_1$, $V_1$ and $\widetilde{V}_1$ all have $r$ columns. Assume also that $2\|E\|_2 < \sigma_r(A)$. Then there exists a matrix $P \in \mathbb{C}^{(m-r)\times r}$ such that the columns of $\widehat{U}_1$, $\widehat{U}_2$, defined by*

$$\widehat{U}_1 = (U_1 + U_2 P)\big(I + P^*P\big)^{-1/2}, \tag{2.13}$$

$$\widehat{U}_2 = \big(U_2 - U_1 P^*\big)\big(I + PP^*\big)^{-1/2}, \tag{2.14}$$

*span $\mathcal{R}(\widetilde{U}_1)$ and $\mathcal{R}(\widetilde{U}_2)$, respectively.*

**Proof.** Following Wedin [20], it is immediate to see that the condition $2\|E\|_2 < \sigma_r(A)$ implies that the sine of the largest canonical angle between $\mathcal{R}(U_1)$ and $\mathcal{R}(\widetilde{U}_1)$ is smaller than one. Thus the cosines of the canonical angles between these subspaces, which are given as the singular values of $\widetilde{U}_1^* U_1$, cannot be zero. The same result applies to the singular values of $\widetilde{U}_2^* U_2$. On the other hand, notice that, for all nonzero $P \in \mathbb{C}^{(m-r)\times r}$, $\widehat{U}_1^*\widehat{U}_1 = I_r$, and therefore the columns of $\widehat{U}_1$ are orthonormal. We thus need to exhibit a matrix $P$ such that $\widehat{U}_1$ defined by (2.13) satisfies $\widetilde{U}_2^*\widehat{U}_1 = 0$. Since this amounts to determining a matrix $P$ such that

$$\widetilde{U}_2^* U_2 P = -\widetilde{U}_2^* U_1, \tag{2.15}$$

existence of $P$ follows because $\widetilde{U}_2^* U_2$ is non singular. Relation (2.14) is immediate. □

Existence of $P$ satisfying (2.13) was first proven by Stewart [22] in the framework of invariant subspaces. He obtained such a $P$ by solving a nonlinear equation via successive approximations, under appropriate conditions. A recast of Stewart's results can be found in [14, Section 8.6]. There the existence of $P$ is ensured provided that $4\|E\|_F < \sigma_r(A)$. Here we show the existence of $P$ by merely imposing acuteness between $\mathcal{R}(U_1)$ and $\mathcal{R}(\widetilde{U}_1)$, which in a sense simplifies the analysis of Stewart.

We are ready to describe the Fourier coefficients of $\tilde{b}$ with respect to bases of $\mathcal{R}(\widetilde{U}_1)$ and $\mathcal{R}(\widetilde{U}_2)$.

**Theorem 1.** *Assume $\widetilde{U}_1$, $\widetilde{U}_2$ as in Lemma* 1, *and $\tilde{b} = b + \varepsilon$, with $b$ in $\mathcal{R}(A)$. Then there exists a unitary matrix $\widetilde{U}' = [\widetilde{U}'_1 \widetilde{U}'_2]$ such that the columns of $\widetilde{U}'_1$ span $\mathcal{R}(\widetilde{U}_1)$, those of $\widetilde{U}'_2$ span $\mathcal{R}(\widetilde{U}_2)$, and*

$$\tilde{u}'^{*}_j \tilde{b} = \begin{cases} \cos(\theta_j) u^{s*}_j b + \tilde{u}'^{*}_j \varepsilon, & 1 \leqslant j \leqslant r, \\ -\sin(\theta_{j-r}) u^{s*}_{j-r} b + \tilde{u}'^{*}_j \varepsilon, & r+1 \leqslant j \leqslant 2r, \\ \tilde{u}'^{*}_j \varepsilon, & 2r+1 \leqslant j \leqslant m, \end{cases} \tag{2.16}$$

*where $\tilde{u}'_j$ is the $j$th column of $\widetilde{U}'$, the $\theta_j$'s are the canonical angles between $\mathcal{S}$ and $\widetilde{\mathcal{S}}$, and $\{u^s_j\}^r_{j=1}$ is a basis of $\mathcal{R}(U_1)$.*

**Proof.** Let the singular value decomposition of $P$ in Lemma 1 be

$$P = \Phi \breve{\Lambda} \Upsilon^* = [\Phi_1 \quad \Phi_2] \begin{bmatrix} \Lambda \\ 0 \end{bmatrix} \Upsilon^*, \tag{2.17}$$

where $\Phi_1$ contains the first $r$ columns of $\Phi$ and $\Lambda$ contains the singular values of $P$ in decreasing order. It then follows that $(I + P^*P)^{-1/2} = \Upsilon \cos\Theta \Upsilon^*$, where $\cos\Theta$ is defined in (2.12), and the singular values of $P$ are the tangents of the canonical angles (see, e.g., Stewart [22]). Replacing $P$ with its SVD in (2.13), and taking the above observations into account, (2.13) can be rewritten as

$$\widetilde{U}'_1 = U^s_1 \cos\Theta + U^o_a \sin\Theta, \tag{2.18}$$

where we set $\widetilde{U}'_1 = \widehat{U}_1 \Upsilon$, $U^s_1 = U_1 \Upsilon$, and $U^o_a = U_2 \Phi_1$. Now define $u^s_j = U^s_1 e_j$, where $e_j$ is the $j$th canonical vector in $\mathbb{R}^m$, and note that $\tilde{u}'^{*}_j \tilde{b} = \tilde{u}'^{*}_j b + \tilde{u}'^{*}_j \varepsilon$. Computing the products $\tilde{u}'^{*}_j b$ in (2.18), we see that (2.16) holds for $j = 1, \ldots, r$, since $U^*_2 b = 0$. Proceeding as before, we see that (2.14) can be rewritten as

$$\widetilde{U}'_2 = \begin{bmatrix} U^o_1 & U^o_2 \end{bmatrix}, \tag{2.19}$$

where $U'_2 = \widehat{U}_2 \Phi$, $U^o_1 = -U^s_1 \sin\Theta + U^o_a \cos\Theta$, and $U^o_2 = \widehat{U}_2 \Phi_2$. Defining $\tilde{u}'_{r+j} = \widetilde{U}'_2 e_j$, for $j = 1, \ldots, m-r$, the remaining inequalities in (2.16) follow from the fact that $U^*_2 b = 0$. □

Notice that, although $\tilde{u}_j$ differs from $\tilde{u}'_j$, the residual norm $\|r_k\|^2_2 = \|Ax_k - \tilde{b}\|^2_2$ can be computed using the coefficients $\tilde{u}'^{*}_j \tilde{b}$ instead of $\tilde{u}^*_j \tilde{b}$, because this residual norm does not depend on the chosen basis. Notice also that, if $\|E\|_2$ is small enough compared with $\sigma_r(A)$, then the coefficients $\tilde{u}'^{*}_j \tilde{b}$, for $j > r$, must be much smaller than those corresponding to $1 \leqslant j \leqslant r$, since $\sin(\theta_j) \approx 0$, in which case the GCV function should be minimized at $k = r$. We can thus conclude that GCV should perform satisfactorily in detecting rank$(A)$ when $\|E\|_2 \ll \sigma_r(A)$. The unclear gap case, which probably happens when $\|E\|_2 \approx \sigma_r(A)$, is difficult to analyze, so we shall resort to numerical simulation.

## 3. Proposed method

We start by reviewing a version of the Conjugate Gradient method for the LS problem $\min \|Ax - b\|$ that avoids explicit computation of the cross-product $A^*A$. It can be described as follows:

**Algorithm CGLS.** Given an initial guess $x^{(0)}$, set

- $r^{(0)} = b - Ax^{(0)}$,
- $p^{(0)} = s^{(0)} = A^* r^{(0)}$,
- $\gamma_0 = \|s^{(0)}\|_2^2$,
- for $k = 0, 1, 2, \ldots$

$$\begin{aligned}
q^{(k)} &= Ap^{(k)}, \\
\alpha_k &= \gamma_k / \|q^{(k)}\|^2, \\
x^{(k+1)} &= x^{(k)} + \alpha_k p^{(k)}, \\
r^{(k+1)} &= r^{(k)} - \alpha_k q^{(k)}, \\
s^{(k+1)} &= A^* r^{(k+1)}, \\
\gamma_{k+1} &= \|s^{(k+1)}\|_2^2, \\
\beta_k &= \gamma_{k+1} / \gamma_k, \\
p^{(k+1)} &= s^{(k+1)} + \beta_k p^{(k)}.
\end{aligned}$$

**End of algorithm.**

The convergence properties of Algorithm CGLS are well-known and may be derived from the observation that the $k$th iterate, $x^{(k)}$, can be defined as the unique solution of the problem

$$\min \|Ax - b\|_2 \quad \text{constrained to } x \in \mathcal{K}_k\big(A^*A, A^*b\big), \tag{3.20}$$

where $\mathcal{K}_k(A^*A, A^*b) = \operatorname{span}\{A^*b, (A^*A)A^*b, \ldots, (A^*A)^{k-1}A^*b\}$ is the Krylov subspace associated with the normal equations. CGLS is interesting because it captures the components of the solution associated with the largest singular values in the early iterates [5, Section 7.4]. Apart from this, for the significant case where the coefficient matrix is exactly rank-deficient, CGLS converges in at most $r$ iterations, where $r = \operatorname{rank}(A)$ [5, Section 7.4], [19]. This is stated in the following theorem.

**Theorem 2.** *Let $x^{(k)}$ $k \geqslant 0$ be the sequence of CGLS iterates related to the LS problem* $\min \|Ax - b\|$. *Then, provided $x^{(0)} \in \mathcal{R}(A^*)$, e.g., $x^{(0)} = 0$, the sequence $x^{(k)}$ converges to the minimum norm solution $x^\dagger = A^\dagger b$, and convergence occurs in at most $r$ steps, where $r = \operatorname{rank}(A)$.*

We emphasize that, although exactly rank-deficient problems rarely occur in practice, there are circumstances where the statement of the theorem is approximately satisfied in the sense that convergence is reached in approximately $r$ steps. Such is the case, for example, when the data matrix satisfies the low-rank-plus-shift structure (see, Golub and Van Loan [14, p. 530]). Another instance is when the singular spectrum of $\widetilde{A}$ presents a well-defined gap between $\tilde{\sigma}_r$ and $\tilde{\sigma}_{r+1}$ [18]. For these cases, both the iterate norm and the residual norm stagnate at some stage of the iterations and convenient stopping criteria, such as the L-curve criterion, are available; see Hansen [18] for details.

The case where the gap is unclear is more difficult to analyze since one is not able to assess the accuracy of the CGLS iterates $x^{(k)}$ step by step. As a consequence, it becomes difficult to stop the algorithm so as to construct satisfactory approximate solutions. Thus the algorithm we propose shall exchange (at a first stage) the problem of constructing satisfactory approximate solutions to P1 using CGLS alone for that of capturing underlying information associated with the singular values of interest.

This can be explained as follows. Recall that the residual vectors $\tilde{s}^{(k)} = \widetilde{A}^*(\widetilde{A}\tilde{x}^{(k)} - \tilde{b})$ are orthogonal. Let $\hat{s}^{(k)}$ be the residual vector $\tilde{s}^{(k)}$ normalized to unit length and define

$$\widetilde{T}_k = \widetilde{S}_k^* \widetilde{A}^* \widetilde{A} \widetilde{S}_k \in \mathbb{C}^{k\times k}, \quad \text{where } \widetilde{S}_k = \left[\hat{s}^{(0)} \ldots \hat{s}^{(k-1)}\right]. \tag{3.21}$$

The matrix $\widetilde{T}_k$ is tridiagonal Hermitian and its entries are easy to compute during the CGLS procedure, see, e.g., [14, p. 528]. Furthermore, it is closely connected with the Lanczos tridiagonalization procedure of $\widetilde{A}^*\widetilde{A}$, so its spectrum concentrates information concerning the largest singular values of $\widetilde{A}$. In connection with CGLS, provided that $x^{(0)} = 0$, it is easy to see from (3.20) that the CGLS iterate $x^{(k)}$ can be computed as

$$x^{(k)} = \widetilde{S}_k \widetilde{T}_k^{-1} \rho e_1^{(k)}, \quad \rho = \|A^* b\|_2,\ e_1^{(k)} = [1, 0, \ldots, 0]^{\mathrm{T}} \in \mathbb{R}^k. \tag{3.22}$$

Let $\widetilde{T}_k = \Psi_k \Lambda_k \Psi_k^*$ be the SVD of $\widetilde{T}_k$, with $\Lambda_k = \operatorname{diag}(\tau_1^{(k)}, \tau_2^{(k)}, \ldots, \tau_k^{(k)})$ and $\Psi_k = [\psi_1^{(k)} \psi_2^{(k)} \cdots \psi_k^{(k)}]$. The eigenvalues $\tau_i^{(k)}$, called *Ritz values*, approximate extreme eigenvalues of $\widetilde{A}^*\widetilde{A}$, whereas the vectors $\widetilde{S}_k \psi_i^{(k)}$, called *Ritz vectors*, approximate the corresponding eigenvectors, see, e.g., [18, Section 6.4]. In terms of the SVD, (3.22) becomes

$$x^{(k)} = \widetilde{S}_k \Psi_k \Lambda_k^{-1} \Psi_k^* \rho e_1^{(k)} = \sum_{i=1}^{k} \frac{\rho \psi_i^{(k)*} e_1^{(k)}}{\tau_i^{(k)}} \widetilde{S}_k \psi_i^{(k)}. \tag{3.23}$$

Thus as more of the required singular values are captured, the information of interest is better contained in $x^{(k)}$. There exists, however, the inconvenience that unwanted information due to small Ritz values is also included in $x^{(k)}$. Therefore, criteria to filter out the contributions of small Ritz values are needed. We address this issue by using the GCV technique.

Algorithm CGLS-GCV combines $p$ steps of CGLS with GCV applied to the projected problem

$$\min \left\| \widetilde{T}_p x - \rho e_1^{(p)} \right\|_2, \tag{3.24}$$

and then uses the minimizer of the related GCV function as a rank estimate for solving problems P1 and P2. Number $p$ is a parameter to be estimated according to criteria which depend on the application under study. Behind CGLS-GCV are some facts which we now discuss shortly. First, notice that the related GCV function becomes

$$G(\ell, p) = \left(\frac{1}{p-\ell}\right) \frac{\sum_{i=\ell+1}^{p} |\rho \psi_i^{(p)*} e_1^{(p)}|^2}{p-\ell}, \quad \ell = 1, \ldots, p-1. \tag{3.25}$$

Hence all information required to compute $G(\ell, p)$ is obtained from the first row of $\Psi_p$. If $p$ is large enough so that all wanted singular values are in $\lambda(\widetilde{T}_p)$, Ritz vectors associated with the $r$ largest Ritz values become right singular vectors, and the remaining Ritz vectors become vectors in $\widetilde{\mathcal{S}}'^{\perp}$. Here $\widetilde{\mathcal{S}}'$ denotes the subspace spanned by right singular vectors associated with the $r$ largest singular values of $\widetilde{A}$. Using the notation of (2.10), this means that

$$\widetilde{S}_p \psi_i^p = \begin{cases} \tilde{v}_i, & 1 \leqslant i \leqslant r, \\ \tilde{w}_i \in \operatorname{span}\{\tilde{v}_1, \ldots, \tilde{v}_r\}^{\perp}, & r+1 \leqslant i \leqslant p. \end{cases} \tag{3.26}$$

Since $\rho \widetilde{S}_k e_1^{(p)} = \widetilde{A}^* \tilde{b}$ implies that $|\rho \psi_i^{(p)*} e_1^{(p)}| = |(\widetilde{S}_p \psi_i^p)^* (\widetilde{A}^* \tilde{b})|$, the GCV function $G(\ell, p)$ actually evaluates the components of $\widetilde{A}^* \tilde{b}$ on Ritz vectors.

We thus conclude that if the $r$ singular values of interest are in $\lambda(\widetilde{T}_p)$ and if $\widetilde{A}^*\tilde{b}$ has components that do not vary much along Ritz vectors associated with unwanted Ritz values, in accordance with what we deduced in Section 2 regarding the application of GCV to rank-deficient problems, we may expect $G(\ell, p)$ to be minimized at $\ell = r$. Two observations concerning numerical issues related to CGLS must be made. The first is that numerical difficulties may arise due to the fact that in inexact arithmetic the residual vectors $\tilde{s}_k$ lose orthogonality. The cure is to use selective or complete reorthogonalization, but extra work is needed. Notice, however, that, if only a few of the largest singular values are required, the extra work spent with reorthogonalization is not substantial [10,27]. The second observation is that, although CGLS avoids explicit computations of cross-products $\widetilde{A}^*\widetilde{A}$, squaring the condition number of $\widetilde{A}$ cannot be avoided. This may result in a loss of accuracy in the smaller singular values. Fortunately, the squaring effect is not that serious when larger singular values are required, see, e.g., [5, p. 81].

We now formally describe our algorithm.

**Algorithm CGLS-GCV.**

1. Setting $\tilde{x}^0 = 0$, perform $p$ steps of CGLS and construct the tridiagonal matrix $\widetilde{T}_p$ as in (3.21).
2. Compute the SVD of $\widetilde{T}_p$, $\widetilde{T}_p = \Psi_p \Lambda_p \Psi_p^*$, and minimize the related GCV function $G(\ell, p)$.
3. Choose the minimizer $k^*$ of the GCV function as the rank of the unperturbed matrix, i.e., set $r = k^*$, and partition $\Psi_p = [\Psi_1 \Psi_2]$, $\Lambda = \operatorname{diag}(\Lambda_1, \Lambda_2)$ with $\Psi_1 \in \mathbb{C}^{n\times r}$ and $\Lambda_1 \in \mathbb{C}^{r\times r}$.
4. Set
   - $\mathcal{R}(\widetilde{S}_p \Psi_1)$ as an approximate solution to P2, and
   - $\tilde{x} = \widetilde{S}_p \Psi_1 \Lambda_1^{-1} \Psi_1^* \beta_1 e_1$ as an approximate solution to P1.

**End of Algorithm.**

Some comments on attributes or limitations of CGLS-GCV are appropriate. In fact, notice that in the absence of noise, because of Theorem 2, CGLS alone solves P1 in exactly $r$ iterations, in which case the GCV technique is not required. Solving P2 is also immediate in this case: it is sufficient to take $\mathcal{S} = \operatorname{span}\{s^{(0)}, \ldots, s^{(r-1)}\}$, where $s^{(k)} = A^*(b - Ax^{(k)})$. Another situation where CGLS-GCV is guaranteed to efficiently solve P1 and P2 is when the data matrix approximately satisfies the low-rank-plus-shift structure (1.2), since in this case, CGLS "almost converges" after $r$ steps [14, p. 530], and, as discussed in Section 2, GCV should correctly estimate $\operatorname{rank}(A)$. However, very little can be said about the behavior of CGLS-GCV for general $A$, as the convergence behavior of CGLS depends on the way the singular values are distributed. That is, slow convergence may occur under certain circumstances. Despite this, since CGLS tends to quickly pick out the components of the solution associated with the largest singular values, even in the unclear gap case [9], extremely slow convergence should not happen in our context.

A brief comment concerning the decision of when to stop CGLS is in order. This decision is problem dependent and very difficult to implement for general rank-deficient problems. But, if sufficient information on the problem under analysis (or its solution) is available, convenient stopping rules can be developed, see, e.g., [15]. Concerning CGLS-GCV, notice that there are two obvious circumstances under which the algorithm may yield inaccurate solutions. The first, when the wanted Ritz pairs are not captured, and the second, when GCV fails in estimating $\operatorname{rank}(A)$. The former can happen because CGLS was stopped too soon, and the cure would be to exploit prior knowledge in order to stop CGLS adequately.

The latter is difficult to predict as the minimizer of the GCV function depends on the components of $\widetilde{A}^*\tilde{b}$ on Ritz vectors, and because these components depend on the amount and nature of noise in the data.

### *3.1. A stopping criterion for CGLS in harmonic retrieval*

We shall now discuss how to adequately stop the CGLS iterations in the framework of harmonic retrieval. Matrices in this area are usually structured (e.g., Hankel or Toeplitz), with entries that are samples of multi exponential signals. Problem P1 is referred to as a *linear prediction problem*, the solution to P2, the row subspace $\mathcal{R}(A^*)$, is known as *signal subspace*, and $r = \operatorname{rank}(A)$ represents the number of frequency components of the solutions. Recall that the goal here is not to construct reasonable approximate solutions to P1 using CGLS, but rather to stop CGLS at some iteration where, at least to our purpose, the underlying signal information associated with the largest singular values of $\widetilde{A}$ is captured.

For our description we link again the CGLS algorithm with $x^{(0)} = 0$ and the Lanczos tridiagonalization procedure applied to $\widetilde{A}^*\widetilde{A}$ with starting vector $\widetilde{A}^*\tilde{b}$, and observe that the Lanczos procedure tends to capture the largest singular values in their natural order in few iterations, as long as the starting vector has strong components along the associated singular vectors [18, Section 6.3].

Our proposal relies on two facts. The first is that in harmonic retrieval, under conditions that are often met in practice, namely $\|E\|_2 < \sigma_r(A)$ and $\|b\|_2 < \|e\|_2$ (which means that the noise does not dominate the signal), our starting vector $\widetilde{A}^*\tilde{b}$ is usually rich enough in signal information (i.e., the strongest components $|\tilde{v}_i^*(\widetilde{A}^*\tilde{b})|$ are associated with $i \leqslant r$).

The second fact is that $\operatorname{rank}(A)$ can be estimated during the CGLS procedure. This can be explained as follows. Note that every $\tilde{x}^{(k)}$ computed during the CGLS procedure may be analyzed for its frequency content: typically, these $\tilde{x}^{(k)}$ contain more and more high frequency components as iterations proceed, diverging quickly after the components associated with large singular values have been found. In practice, this can be seen by examining the number of frequency peaks in the Fourier spectrum of $\tilde{x}^{(k)}$. For data free of noise, the author's experience is that the number $r$ of peaks corresponding to the frequency components of the solution $x^\dagger$ is detected very early and remains unmodified until convergence is obtained. This can be seen in Fig. 1(f)–(e), where we display the behavior of the CGLS iterates for a linear prediction problem from magnetic resonance spectroscopy.

The only observed effect of CGLS iterates in the frequency domain is an alteration of the height and width of these peaks but not of their number or position. We believe that this behavior is because all successive $x^{(k)}$ belong to the $r$-dimensional signal subspace $\mathcal{R}(A^*)$. On the other hand, the behavior of the CGLS iterates dramatically changes when noise is present in the data: if, at early iterations, the number of meaningful frequency peaks is nearly identical to that observed in the noise free case, it suddenly increases considerably when the noise starts contaminating the computed iterate (see Fig. 1(c)–(f)). Numerical examples in harmonic retrieval and image reconstruction illustrating this phenomenon can be seen in [4,16]. We thus conclude that $\operatorname{rank}(A)$ may be estimated by counting meaningful peaks of the Fourier spectrum of some $\tilde{x}^{(k)}$ of the very first iterations.

Based on these two facts and assuming that an estimate for $\operatorname{rank}(A)$ is available, we propose to stop CGLS after $p$ steps, where $p$ is slightly larger than twice the estimate for $\operatorname{rank}(A)$. This choice of $p$ agrees with common numerical experience of some authors, see, e.g., [10,27], who concluded that, in general, $2 \times r$ Lanczos iterations are sufficient to construct good approximations to the $r$ largest singular values of perturbations of rank-$r$ Toeplitz matrices. As for the estimate of $\operatorname{rank}(A)$, we propose to compute the Fourier spectrum of the second CGLS iterate and then to choose as rank estimate the number of

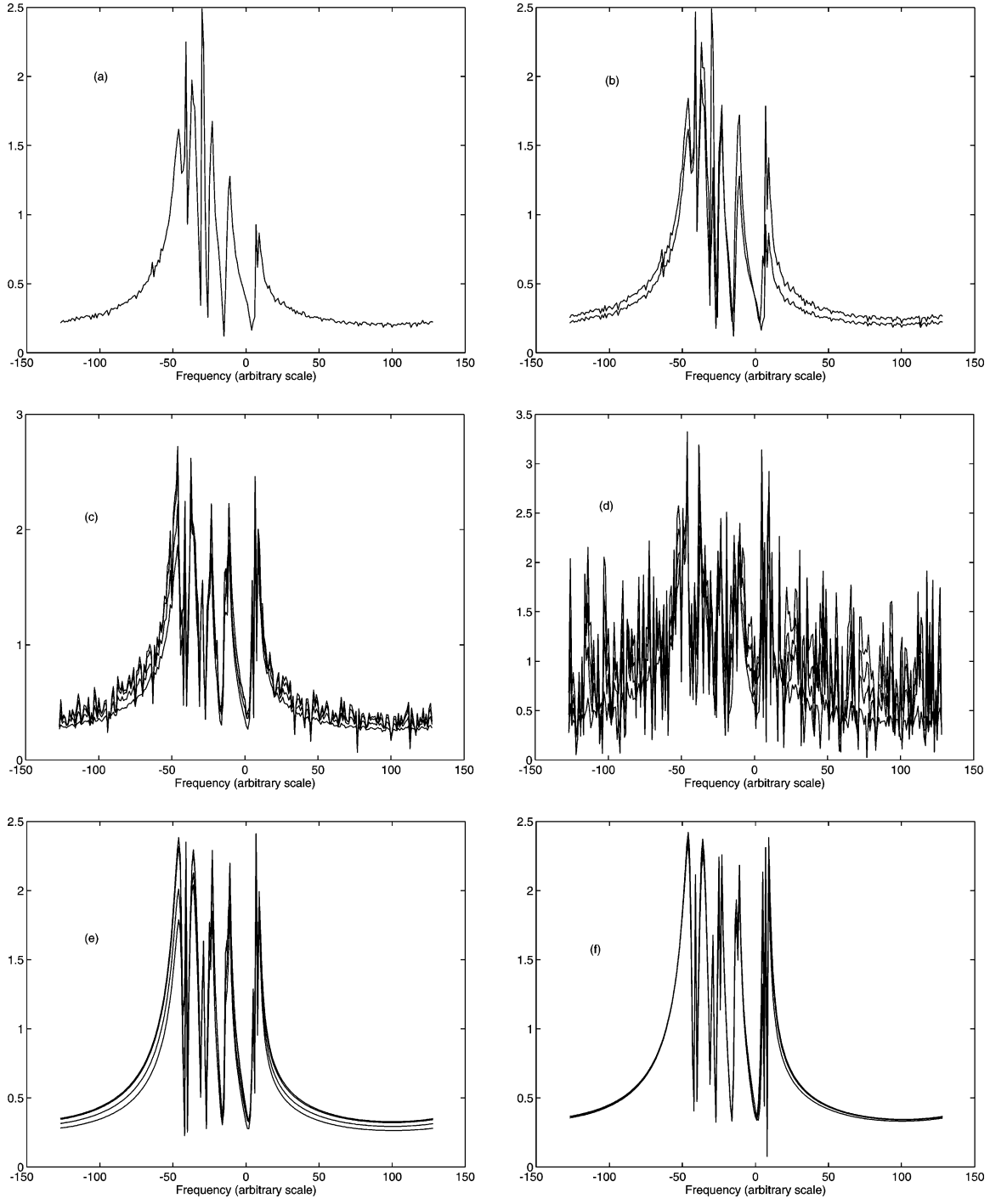


Fig. 1. Behavior of CGLS iterates in frequency domain from MRS (signal parameters are in Table 1, next section). Iterates using perturbed data: (a) $k = 1$, (b) $k = 1 : 2$, (c) $k = 3 : 6$, (d) $k = 7 : 10$. Iterates using clean data: (e) $k = 3 : 6$, (f) $k = 7 : 10$.

dominant peaks of that spectrum. The choice of the second iterate to estimate rank$(A)$ is motivated by the observation that, depending on the amount of noise on the data, irrelevant small peaks start to appear from the third or fourth iteration on. Obviously, there may exist many ways to decide whether a peak is dominant or not. Our choice has been to accept frequency peaks as dominant when they level off a predetermined threshold value. To determine the threshold value in practice, the relative maximums of the corresponding spectrum should be computed to locate the frequency peaks. Once this is done, the threshold value can be chosen as a fraction of the maximum peak. Numerous numerical experiments in modal parameter identification and MRS have shown that a threshold value equal to (maximumpeak)/3 yields good results.

## 4. Numerical experiments

*An example from magnetic resonance spectroscopy (MRS).* In this section we illustrate the performance of CGLS-GCV on the solution of problems P1 and P2 arising in harmonic retrieval. In applications like this, the data matrix $\widetilde{A}$ has Hankel structure and its entries are defined by $\tilde{a}_{i,j} = \tilde{h}_{i+j-1}$, where $\tilde{h}_k = h_k + \varepsilon_k$ are samples of a perturbed signal. Problem P1 consists of computing approximations to a backward prediction problem $\min \|Ax - b\|$, where $A$ and $b$ contain samples of pure signal $h_k$, with $b = [h_0, \ldots, h_{m-1}]^T$. Problem P2 addresses the computation of approximations of the subspace $\mathcal{R}(A^*)$. For details on applications in MRS, see [8]. Our implementation of CGLS-GCV relies on slight modifications of functions *cgls* (with complete reorthogonalization) and *gcv* from the Matlab regularization tools by Hansen [17]. For comparison, we also solve P1 and P2 using *lurv_a* and *lulv_a*, two low-rank-revealing (LRR) algorithms from the Matlab templates by Fierro et al. [12]. In the latter case rank$(A)$ was provided a priori.

The signal $h_k$ comes from an *in vivo* $^{31}P$ spectrum measured in a human brain and given as

$$h_k = \sum_{j=1}^{11} c_j e^{\imath\phi_j} e^{(\alpha_j + \imath\omega_j)k\Delta t}, \quad \imath = \sqrt{-1},\ k = 0, 1, \ldots, 511, \tag{4.27}$$

Table 1
Exact parameter values for the MRS signal

| Peak $j$ | $c_j$ | $\xi_j$ (degrees) | $\alpha_j$ | $w_j/2\pi$ (Hz) |
|---|---|---|---|---|
| 1 | 75 | 135 | 50 | −86 |
| 2 | 150 | 135 | 50 | −70 |
| 3 | 75 | 135 | 50 | −54 |
| 4 | 150 | 135 | 50 | 152 |
| 5 | 150 | 135 | 50 | 168 |
| 6 | 150 | 135 | 50 | 292 |
| 7 | 150 | 135 | 50 | 308 |
| 8 | 150 | 135 | 25 | 360 |
| 9 | 1400 | 135 | 285 | 440 |
| 10 | 60 | 135 | 25 | 490 |
| 11 | 500 | 135 | 200 | 530 |

where $\Delta t = 0.000333$ and $\phi_j = \xi_j \pi/180$. The other parameters are given in Table 1. The unperturbed matrix $A$ is therefore of rank 11. Because the signal includes closely spaced components $z_j = e^{(\alpha_j + \imath\omega_j)k\Delta t}$ in the time domain, which are displayed as closely overlapping thin peaks in the frequency domain (see Fig. 2), the signal is very sensitive to noise [1,3]; in practice it represents a difficult test case for identification algorithms [23]. Solutions to either P1 or P2 are often used to estimate the signal parameters from noisy data.

In order to investigate the performance of GCLS-CGV we used a matrix $\widetilde{A}$ of order $128 \times 128$, a vector $\tilde{b} = [\tilde{h}_0,\ \tilde{h}_1, \ldots, \tilde{h}_{127}]^{\mathrm{T}}$, and ran 100 random realizations (with the seed value of the random generator set to zero) using Gaussian noise with standard deviation on both real and imaginary parts equal to 15.

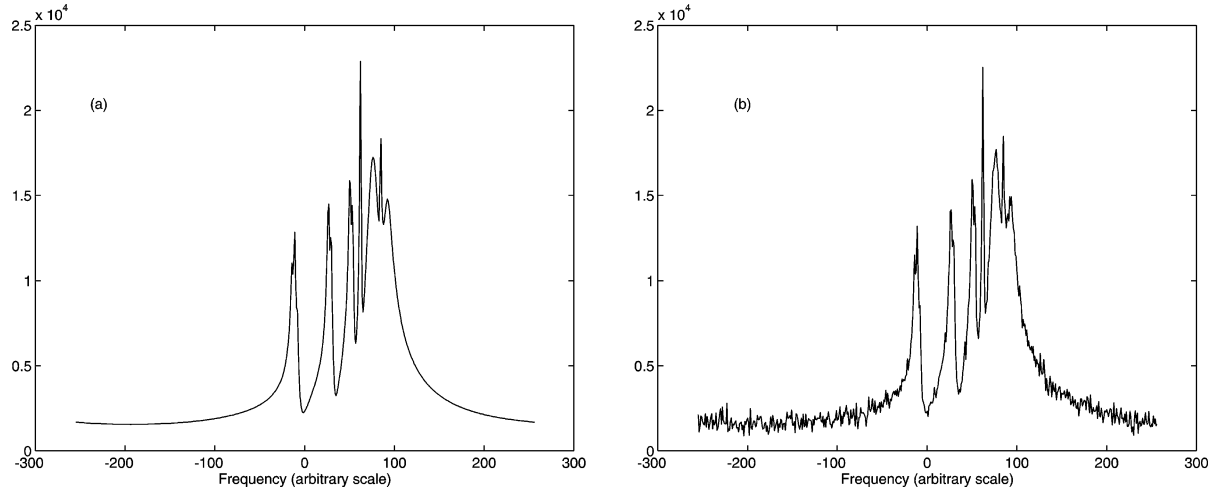


Fig. 2. Fourier spectrum of MRS signals: (a) clean data; (b) perturbed data.

Table 2
Singular values of data matrices of dimension $m = n = 128$

| $j$ | $\sigma_j \times 10^{-3}$ | $\tilde{\sigma}_j \times 10^{-3}$ | $\hat{\sigma}_j \times 10^{-3}$ | $\tilde{\sigma}_j \times 10^{-3}$ | $\hat{\sigma}_j \times 10^{-3}$ |
|---|---|---|---|---|---|
| 1 | 8.553584 | 8.576484 | 8.576484 | 8.590613 | 8.590613 |
| 2 | 6.743550 | 6.777738 | 6.777738 | 6.727226 | 6.727226 |
| 3 | 5.804921 | 5.776895 | 5.776895 | 5.756752 | 5.756752 |
| 4 | 5.120707 | 5.152361 | 5.152361 | 5.184471 | 5.184471 |
| 5 | 4.734389 | 4.775110 | 4.775110 | 4.718573 | 4.718573 |
| 6 | 2.443993 | 2.355343 | 2.355343 | 2.491402 | 2.491402 |
| 7 | 1.678095 | 1.726428 | 1.726428 | 1.679051 | 1.679051 |
| 8 | 1.521250 | 1.593807 | 1.593807 | 1.509216 | 1.509216 |
| 9 | 1.412832 | 1.448948 | 1.448948 | 1.439113 | 1.439113 |
| 10 | 0.980690 | 0.789505 | 0.789505 | 0.811810 | 0.811810 |
| 11 | 0.714847 | 0.578135 | 0.578135 | 0.682790 | 0.682790 |
| 12 | 0.000000 | 0.536610 | 0.536610 | 0.613084 | 0.613084 |
| 13 | 0.000000 | 0.481352 | 0.481353 | 0.484427 | 0.484046 |
| 14 | 0.000000 | 0.424903 | 0.415401 | 0.471570 | 0.468845 |
| 15 | 0.000000 | 0.415245 | 0.380197 | 0.453056 | 0.439401 |

Singular values of $A$ and $\widetilde{A}$ are denoted by $\sigma_j$ and $\tilde{\sigma}_j$ respectively. Approximations of $\tilde{\sigma}_j$ from $\widetilde{T}_p$ in (3.21) are denoted by $\hat{\sigma}_j$ and were obtained using $p = 20$ CGLS iterations. The standard deviation value was chosen in such a way that the singular spectrum of $\widetilde{A}$ presents no distinct gap between $\tilde{\sigma}_{11}$ and $\tilde{\sigma}_{12}$, as illustrated in Table 2 (columns 3 and 4) for a typical run.

The rank detection task was done using a restricted GCV function $\widehat{G}(\ell, p)$ employing only 18 coefficients. Results of the experiment displayed in Fig. 3 show a failure rate of 3%. Failures occurred because the random noise produced, in each "bad run," a rather "favorable" gap between $\tilde{\sigma}_{12}$ and $\tilde{\sigma}_{13}$, that induced the GCV function to be minimized at $k = 12$. This is illustrated in columns 5 and 6 of Table 2, which contain the first 15 singular values $\tilde{\sigma}_j$ and their approximations $\hat{\sigma}_j$, for the first "bad run." We also tried a GCV function using all 20 coefficients. The results obtained resembled those of the restricted case, see Fig. 4, but the failure rate increased to 5%.

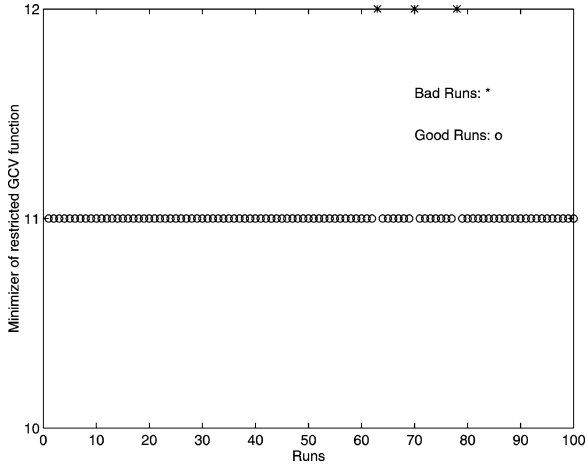


Fig. 3. Performance of CGLS-GCV in detecting rank($A$).

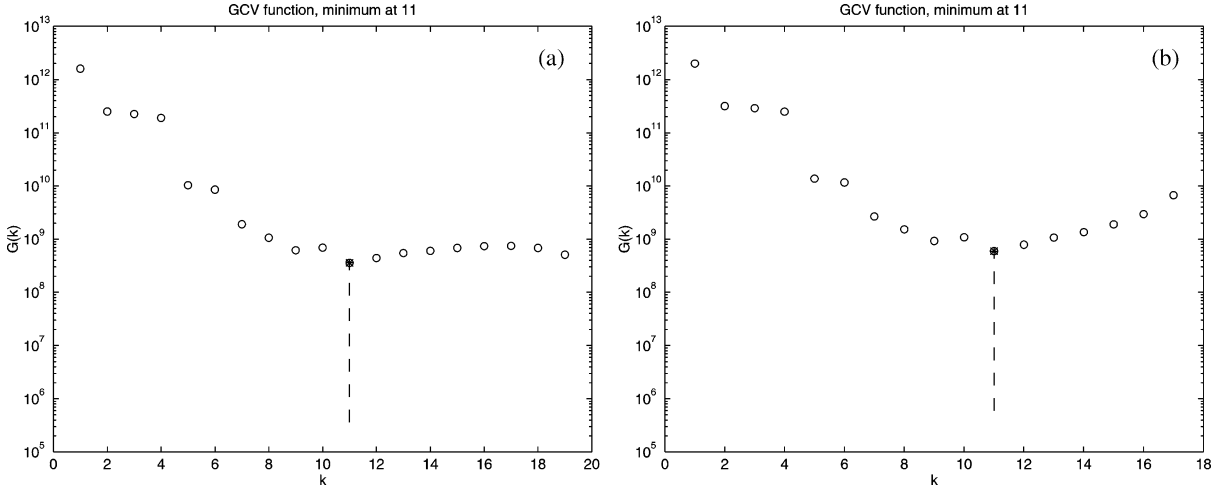


Fig. 4. Behavior of GCV function: (a) unrestricted case; (b) restricted case.

Table 3
Results on accuracy of solutions to P1 and P2 obtained by three different methods

| Accuracy results to P1 | | Accuracy results to P2 | |
|---|---|---|---|
| $\|x_{\mathrm{EXACT}} - \tilde{x}_{\mathrm{SVD}}\|$ | 0.074206 | $\mathrm{d}(\mathcal{S}', \widetilde{\mathcal{S}}'_{\mathrm{SVD}})$ | 0.118338 |
| $\|x_{\mathrm{EXACT}} - \tilde{x}_{\mathrm{GCV}}\|$ | 0.074206 | $\mathrm{d}(\mathcal{S}', \widetilde{\mathcal{S}}'_{\mathrm{GCV}})$ | 0.118338 |
| $\|x_{\mathrm{EXACT}} - \tilde{x}_{\mathrm{LRR}}\|$ | 0.074316 | $\mathrm{d}(\mathcal{S}', \widetilde{\mathcal{S}}'_{\mathrm{LRR}})$ | 0.118931 |

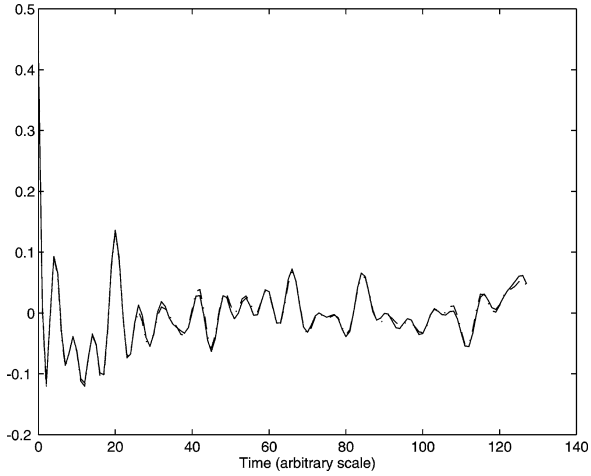


Fig. 5. Real part of exact solution to P1 (solid line). Real part of approximate solution to P1 constructed by CGLS-GCV method (dash-dotted line).

The approximate solution to P1 constructed by CGLS-GCV is depicted in Fig. 5. Approximate solutions to P1 using LRR algorithms as well as the SVD of $\widetilde{A}$ were also constructed. They are denoted by $\tilde{x}_{\mathrm{GCV}}$, $\tilde{x}_{\mathrm{LRR}}$, and $\tilde{x}_{\mathrm{SVD}}$, respectively, and their accuracy measured by comparing them with the exact solution $x_{\mathrm{EXACT}}$. Results displayed in Table 3 show that GCLS-GCV yields better results than the tested LRR algorithms (both LRR algorithms produced similar results).

Approximate solutions to problem P2 using CGLS-GCV, LRR decompositions, and the SVD of $\widetilde{A}$, are denoted by $\widetilde{S}'_{\mathrm{GCV}}$, $\widetilde{S}'_{\mathrm{LRR}}$, and $\widetilde{S}'_{\mathrm{SVD}}$, respectively. Results on the accuracy of the computed approximate solutions to both P1 and P2, are presented in Table 3.

In order to compare the computational costs of the various algorithms considered when solving P2, we compute the ratio of the flops needed by SVD to that required by LRR and CGLS-GCV. Results of the computations presented in Table 4 reveal that CGLS-GCV is faster than both techniques SVD and LRR. In particular, it is seen that CGLS-GCV is approximately 4 times faster than the tested LRR algorithms, and that this ratio can increase with the dimension of the data matrix.

Finally, to investigate the performance of CGLS-GCV as a function of the parameter $p$, we repeatedly applied the algorithm to the same problem, using different values of $p$. The rank detection task was addressed using a GCV function based on all coefficients if $p \leqslant 18$, and 18 coefficients if $p \geqslant 20$. Results shown in Table 5 are eloquent. The quality of the approximate solutions to P1 and P2 were satisfactory only for $p \geqslant 18$. Carrying out the analysis of the GCV function based on all $p$ coefficients for $p > 20$, we

Table 4
Ratio of Flops counts (in MATLAB) needed to solve P2

| Dimension | 128 | 256 |
|---|---|---|
| $\frac{\text{Flops}_{\text{SVD}}}{\text{Flops}_{\text{LRR}}}$ | 6.654339 | 12.976454 |
| $\frac{\text{Flops}_{\text{SVD}}}{\text{Flops}_{\text{GCV}}}$ | 26.533674 | 59.407042 |

Table 5
Performance of GCLS-GCV in detecting rank($A$) for several values of $p$

| $p$ | Failure rate (%) | $p$ | Failure rate (%) |
|---|---|---|---|
| 14 | 8 | 20 | 3 |
| 16 | 5 | 22 | 2 |
| 18 | 5 | 24 | 2 |

obtained results that did not resemble so much those results obtained with 18 coefficients. For instance, for the case $p = 22$, the failure rate increased to 25%.

## 5. Conclusions

In this work we presented an algorithm for solving two important rank-deficient problems appearing frequently in practical applications and illustrated its performance by means of numerical experiments involving rank-deficient problems arising in harmonic retrieval. The algorithm's main attribute is the satisfactory detection of the rank of the matrix associated to the unperturbed problem, even if the singular spectrum of the data matrix presents no clear gap. Rank detection was accomplished by minimizing a GCV function related to a small $p \times p$ projected LS problem, with $p$ easy to estimate (in harmonic retrieval), and the algorithm was successful in almost all numerical experiments. However, more research is needed to investigate the influence of $p$ on the minimizer of the GCV function. Similarly, the influence of $p$ on the convergence of Ritz values to desired eigenvalues needs to be investigated. Apart from this, although the algorithm was shown to significantly outperform both the SVD-based and two RR-based approaches, we are aware that more experience on the behavior of the algorithm is needed when applied to rank-deficient problems arising from other areas. Further, we emphasize that a more efficient variant of GCLS-GCV can be obtained when the data matrix has some structure such as Hankel or Toeplitz; the same comment applies to RR algorithms. This is always possible since matrix–vector products can be efficiently carried out by using the Fast Fourier Transform technique. A LRR-based algorithm where this is done is reported in [26]. There the data matrix is Toeplitz of order $257 \times 256$ and the dimension of the wanted subspace is 10. Under these conditions, the LRR algorithm was about 56 times faster than the SVD. This no longer outperforms the results of CGLS-GCV using conventional matrix–vector products, as shown in Table 4. Even more experience with other LRR algorithms is needed. Other hybrid methods obtained by substituting CGLS by iterative methods such as LSQR or GMRS should be tested to solve rank-deficient problems. This is the subject of ongoing work.

## Acknowledgements

The author wishes to thank the referees for their careful reading of the paper and for their constructive criticism.

## References

[1] F.S.V. Bazán, Conditioning of rectangular Vandermonde matrices with nodes in the unit disk, SIAM J. Matrix Anal. Appl. 21 (2000) 679–693.
[2] F.S.V. Bazán, C. Bavastri, An optimized pseudo-inverse algorithm (OPIA) for multi-input multi-output modal parameter identification, Mech. Syst. Signal Process. 10 (1996) 365–380.
[3] F.S.V. Bazán, Ph.L. Toint, Conditioning of infinite Hankel matrices of finite rank, Systems Control Lett. 41 (2000) 347–359.
[4] F.S.V. Bazán, Ph.L. Toint, M.C. Zambaldi, A conjugate-gradient based method for harmonic retrieval problems that does not use explicit signal subspace computation, Technical Report 16, Department of Mathematics, FUNDP, Namur, Belgium, 1997.
[5] Å. Björk, Numerical Methods for Least Squares Problems, SIAM, Philadelphia, PA, 1996.
[6] Å. Björk, E. Grimme, P. Van Dooren, An implicit shift bidiagonalization algorithm for ill-posed problems, BIT 34 (1994) 510–534.
[7] C.F. Cremona, H.A. Brandon, Model order testing in discrete time domain identification methods, Mech. Syst. Signal Process. 6 (1992) 229–236.
[8] R. de Beer, D. van Ormondt, Analysis of NMR data using time domain fitting procedures, in: M. Rudin, J. Seelig (Eds.), NMR Basic Principles and Progress, Vol. 26, Springer, Berlin, 1997, pp. 201–248.
[9] A. Van der Sluis, The convergence behaviour of conjugate gradients and Ritz values in various circumstances, in: R. Beauwens, P. de Groen (Eds.), Iterative Methods in Linear Algebra, Elsevier, New York, 1992, pp. 49–66.
[10] L. Elden, E. Sjöstrom, Fast computation of signal subspace, Signal Process. 210 (1994) 763–776.
[11] R. Fierro, L. Vanhamme, S. Van Huffel, Total least squares algorithms based on rank-revealing complete orthogonal decompositions, in: S. Van Huffel (Ed.), Recent Advances in Total Least-Squares Techniques and Errors-in-Variables Modelling, SIAM, Philadelphia, PA, 1997, pp. 99–116.
[12] R.D. Fierro, P.C. Hansen, P.S.K. Hansen, UTV tools: Matlab templates for rank-revealing UTV decompositions, Numer. Algorithms 20 (1999) 165–194.
[13] G.H. Golub, M.T. Heath, G. Wahba, Generalized cross-validation as a method for choosing a good ridge parameter, Technometrics 21 (1979) 215–223.
[14] G.H. Golub, C.F. Van Loan, Matrix Computations, 3rd Edition, Johns Hopkins University Press, Baltimore, MD, 1996.
[15] M. Hanke, P.C. Hansen, Regularization methods for large-scale problems, Surveys Math. Indust. 3 (1993) 253–315.
[16] M. Hanke, J. Nagy, R. Plemmons, Preconditioned iterative regularization for ill-posed problems, in: L. Reichel, R.S. Varga (Eds.), Numerical Linear Algebra, De Gruyter, Berlin, 1993, pp. 141–163.
[17] P.C. Hansen, Regularization tools, a Matlab package for analysis and solution and solution of discrete ill-posed problems, Numer. Algorithms 6 (1994) 1–35.
[18] P.C. Hansen, Rank-Deficient and Discrete Ill-Posed Problems—Numerical Aspects of Linear Inversion, SIAM, Philadelphia, PA, 1997.
[19] M.R. Hestenes, Pseudoinverses and conjugate gradients, Commun. ACM 18 (1975) 40–43.
[20] Per-Åke Wedin, Perturbation bounds in connection with singular value decomposition, BIT 12 (1972) 99–111.
[21] D.P. O'Leary, J.A. Simmons, A bidiagonalization-regularization procedure for large-scale regularization of ill-posed problems, SIAM J. Sci. Stat. Comput. 2 (1981) 474–489.
[22] G.W. Stewart, Error and perturbation bounds for subspaces associated with certain eigenvalue problems, SIAM Rev. 32 (1973) 727–764.
[23] J. Totz, A. Van Den Boogart, S. Van Huffel, D. Graveron-Demilly, I. Dologlou, R. Heidler, D. Michel, The use of continuous regularization in the automated analysis of MRS time-domain data, J. Magn. Resonance 124 (1997) 400–409.

[24] A. Van Der Veen, E.F. Deprettere, A.L. Swindlehurst, Subspace-based signal analysis using singular value decomposition, Proc. IEEE 81 (1993) 1277–1309.
[25] S. Van Huffel, H. Chen, C. Decanniere, P. Van Hecke, Algorithm for time-domain NMR data fitting based on total least squares, J. Magn. Resonance A 110 (1994) 228–237.
[26] L. Vanhamme, R.D. Fierro, S. Van Huffel, R. de Beer, Fast removal of residual water in proton spectra, J. Magn. Resonance 132 (1998) 197–203.
[27] G. Xu, T. Kailath, Fast estimation of principal eigenspace using Lanczos algorithm, SIAM J. Matrix Anal. Appl. 15 (1994) 974–994.
[28] H. Zha, Z. Zhang, Matrices with low-rank-plus-shift structure: Partial SVD and latent semantic indexing, SIAM J. Matrix Anal. Appl. 21 (1999) 522–536.